AMERICAN JOURNAL OF PHYSIOLOGY
LUNG CELLULAR AND MOLECULAR PHYSIOLOGY

Am J Physiol Lung Cell Mol Physiol 321: L377–L391, 2021.
First published June 9, 2021; doi:10.1152/ajplung.00477.2020

RESEARCH ARTICLE

FAM13A as potential therapeutic target in modulating TGF-β-induced airway tissue remodeling in COPD

Anthony Tam,[1,3] Pascal Leclair,[1] Ling Vicky Li,[2] Chen X. Yang,[3] Xuan Li,[3] Dominik Witzigmann,[4,5] Jayesh A. Kulkarni,[4,5] Tillie-Louise Hackett,[3] Delbert R. Dorscheid,[3] Gurpreet K. Singhera,[3] James C. Hogg,[3] Pieter R. Cullis,[4,5] Don D. Sin,[3] and Chinten James Lim[1]

[1]*Department of Pediatrics, University of British Columbia, Vancouver, British Columbia, Canada;* [2]*Department of Pathology, University of British Columbia, Vancouver, British Columbia, Canada;* [3]*Center for Heart Lung Innovation, University of British Columbia, St. Paul's Hospital, Vancouver, British Columbia, Canada;* [4]*Department of Biochemistry and Molecular Biology, University of British Columbia, Vancouver, British Columbia, Canada; and* [5]*NanoMedicines Innovation Network, Vancouver, British Columbia, Canada*

Abstract

Genome-wide association studies have shown that a gene variant in the Family with sequence similarity 13, member A (FAM13A) is strongly associated with reduced lung function and the appearance of respiratory symptoms in patients with chronic obstructive pulmonary disease (COPD). A key player in smoking-induced tissue injury and airway remodeling is the transforming growth factor-β1 (TGF-β1). To determine the role of FAM13A in TGF-β1 signaling, *FAM13A*$^{-/-}$ airway epithelial cells were generated using CRISPR-Cas9, whereas overexpression of FAM13A was achieved using lipid nanoparticles. Wild-type (WT) and *FAM13A*$^{-/-}$ cells were treated with TGF-β1, followed by gene and/or protein expression analyses. *FAM13A*$^{-/-}$ cells augmented TGF-β1-induced increase in collagen type 1 (COL1A1), matrix metalloproteinase 2 (MMP2), expression compared with WT cells. This effect was mediated by an increase in β-catenin (CTNNB1) expression in *FAM13A*$^{-/-}$ cells compared with WT cells after TGF-β1 treatment. *FAM13A* overexpression was partially protective from TGF-β1-induced COL1A1 expression. Finally, we showed that airway epithelial-specific FAM13A protein expression is significantly increased in patients with severe COPD compared with control nonsmokers, and negatively correlated with lung function. In contrast, β-catenin (CTNNB1), which has previously been linked to be regulated by FAM13A, is decreased in the airway epithelium of smokers with COPD compared with non-COPD subjects. Together, our data showed that FAM13A may be protective from TGF-β1-induced fibrotic response in the airway epithelium via sequestering CTNNB1 from its regulation on downstream targets. Therapeutic increase in FAM13A expression in the airway epithelium of smokers at risk for COPD, and those with mild COPD, may reduce the extent of airway tissue remodeling.

airway epithelium; COPD; FAM13A; lipid nanoparticles; TGF-β1

INTRODUCTION

Previous reports have shown that chronic obstructive pulmonary disease (COPD) is associated with a decline in lung function with symptoms of chronic cough, sputum production, and breathlessness on exertion in ~20% of adults over 40 yr of age (1–3). Recently, genome-wide association studies (GWAS) and large-scale meta-analyses have shown that several genes are reproducibly associated with lung function in patients with COPD (4–9). One of these is the Family with sequence similarity 13, member A (FAM13A), which has been strongly related to reduce lung function and with increased risk of COPD (10–12). In response to repetitive cigarette smoke, it has been shown in COPD that the airway epithelium releases transforming growth factor-β1 (TGF-β1), and is thought to be associated with airway fibrosis and luminal narrowing (13–16). Remodeled airways in COPD demonstrate changes in markers of epithelial-mesenchymal transition (EMT), including increased collagen type 1 (COL1A1), matrix metalloproteinase 2 (MMP2), and vimentin (VIM), and decreased E-cadherin (CDH1), which may be exacerbated by cigarette smoke-induced oxidative stress, leading to overactivity of TGF-β1 (17, 18).

The mechanisms connecting the role of FAM13A and airway tissue remodeling are not well understood. Jiang et al. (19) have shown that FAM13A interacts with protein phosphatase 2A and glycogen synthase kinase 3β for the ubiquitination and degradation of β-catenin (CTNNB1). TGF-β1-induced matrix synthesis in the airway epithelium has been shown to reduce the levels of E-cadherin (CDH1), thereby liberating CTNNB1 from its complex into the cytoplasm (20). Free and unbound CTNNB1, which has not been subjected to proteasomal degradation, can translocate into the nucleus and serve as transcriptional coactivators to its DNA-binding

Correspondence: C. J. Lim (cjlim@mail.ubc.ca); D. D. Sin (Don.Sin@hli.ubc.ca).
Submitted 7 October 2020 / Revised 27 May 2021 / Accepted 2 June 2021

Table 1. *Demographics of subjects with COPD: immunohistological cohort study*

Characteristics	Nonsmoking Controls	COPD, GOLD Stage 2	COPD, GOLD Stages 3 and 4
Sex (male/female)	2/3	6/3	3/5
Smoking status, non/current/ex/NA	5/0/0/0	0/4/3/2	0/1/7/0
Age, yr	59.6 ± 19.8	63.7 ± 9.0	61.0 ± 6.1
%FEV1/FVC	83.0 ± 4.4	57.1 ± 5.6	33.4 ± 11.9

Values are means ± SD or *n*. COPD, chronic obstructive pulmonary disease; FEV1, forced expiratory volume in one second; FVC, forced vital capacity; GOLD, global initiative for chronic obstructive lung disease; NA, not available.

partner, TCF/LEF (T cell factor/lymphoid enhancer factor), to initiate the transcription of CTNNB1-regulated genes (21–24). However, the mechanistic role of FAM13A in modulating the expression of CTNNB1 in TGF-β1-induced EMT responses is not well characterized.

In this study, we used CRISPR-Cas9 gene editing technology in airway epithelial cells to determine the effects of FAM13A on TGF-β1-mediated response, and characterize FAM13A protein expression in human lung tissues from individuals with and without COPD. First, we showed that loss of FAM13A increased TGF-β1-induced rise in COL1A1, MMP2, and CTNNB1 expression in human airway epithelial cells. Disruption of CTNNB1 using gene silencing technology and pharmacological inhibitors consistently decreased TGF-β1-induced rise in *COL1A1* gene expression. Overexpression of FAM13A using lipid nanoparticles decreased TGF-β1-induced rise in COL1A1 protein expression. Finally, we demonstrated that FAM13A expression is upregulated, whereas CTNNB1 expression is downregulated in the airway epithelium of patients with COPD compared with subjects without COPD. Collectively, these data indicate that FAM13A may have a protective role against epithelial remodeling that leads to progressive narrowing of the airways in COPD.

MATERIALS AND METHODS

Human Lung Tissues for Immunohistochemistry

Formalin-fixed paraffin-embedded (FFPE) human lung tissue samples were obtained from five nonsmoking controls, nine smokers with COPD; with global initiative for chronic obstructive lung disease (GOLD) stage 2 (moderate) disease, and eight smokers with GOLD 3 or 4 (severe or very severe). All of these samples were collected following written informed consent from patients undergoing thoracic surgery who donated lung tissues to the University of British Columbia (UBC) James Hogg lung tissue registry located at St. Paul's Hospital approved by the Providence Health Care Research Ethics Board (PHCREB) H00-50110. All experiments on human samples were conducted in accordance with existing guidelines under the PHCREB protocol approved by the University of British Columbia (B17-0027). The previously reported patient demographics are summarized in Table 1 (50).

Immunohistochemistry

FFPE sections of human lung tissues were stained with antibodies against FAM13A (Sigma HPA038109) using the Bond Polymer Refine Red Detection kit on the Leica Bond Autostainer according to the manufacturer's protocol. Slides were cover-slipped and scanned using the Aperio imaging system (Leica Biosystems; Concord, Ontario).

Human Airway Epithelial Gene Expression *Cohort 1*

To provide gene expression evidence of airway epithelial transition in smokers with or without COPD, human small airway epithelial (10th-12th generation bronchi) gene expression data were collected from 16 Gene Expression Omnibus (GEO) microarray studies (GSE19667, GSE5058, GSE11784, GSE11906, GSE8545, GSE10006, GSE20257, GSE11952, GSE63127, GSE13933, GSE4498, GSE18385, GSE17905, GSE13931, GSE19407, and GSE7832). All of these studies were pooled into one cohort as these studies were generated using the same microarray platform (U133A Plus 2.0 array) and reported by the same laboratory. Raw data (.CEL files) downloaded from the GEO were tested for batch effect and outliers using principal component analysis. Since no obvious batch effect was present, the combined data were normalized using the Robust Multi-array Average (RMA) method. After confirmation and removal of three outliers, this cohort contains 68 nonsmokers, 101 smokers, and 42 smokers with COPD. A summary of the patient demographics is presented in Table 2.

Human Airway Epithelial Gene Expression *Cohort 2*

To determine the gene expression directionality of *CTNNB1* in COPD, we used gene expression data of airway epithelia obtained from individuals with and without COPD at the British Columbia Cancer Agency (BCCA; GSE37147). In brief, RNA was obtained from small airways of smokers (with or without COPD) through a research bronchoscopy. These samples were then processed and hybridized to Affymetrix Human Gene 1.0 ST Arrays. A total of 269 arrays from 267 subjects were hybridized. Data from the 269 microarrays were used for RMA normalization. Data from 238 subjects were used in the downstream analysis to determine the relationship of gene expression with COPD-related phenotypes. Raw gene expression from GSE37147 (.CEL files) were downloaded from GEO, and then normalized using the Robust Multichip Average (RMA) algorithm. The association between *CTNNB1* gene expression with FEV1% predicted, FEV1/FVC, COPD, or smoking status was tested in linear regressions adjusted for age, sex, and smoking status. The analyses were done in *R* (3.6.0). The patient

Table 2. *Demographics of nonsmokers, smokers, and smokers with COPD for airway epithelial gene expression analyses (cohort 1)*

Pooled Cohort	Nonsmokers	Smokers	Smokers with COPD
n	68	101	42
Male	42 (61.8%)	68 (67.3%)	31 (73.8%)
Female	26 (38.2%)	33 (32.7%)	11 (26.2%)
Age, yr	39.0 (15.2)	43.0 (8.0)	51.5 (12.5)
Pack years	0.0 (0.0)	24.0 (22.0)	30.5 (26.5)

Values are either number (percentage) or median (interquartile range) where appropriate. COPD, chronic obstructive pulmonary disease.

Table 3. *Demographics of subjects with or without COPD for airway epithelial gene expression analyses (cohort 2)*

GEO No. GSE37147	Current Smokers with COPD	Current Smokers without COPD	Ex-Smokers with COPD	Ex-Smokers without COPD
Total	30	69	57	82
Sex (female)	14 (46.7%)	35 (50.7%)	21 (36.8%)	33 (40.2%)
Sex (male)	16 (53.3%)	34 (49.3%)	36 (63.2%)	49 (59.8%)
Age, yr	63.2 ± 6.7	62.2 ± 6.0	66.1 ± 5.6	65.8 ± 5.0
%FEV1/FVC	56.9 ± 11.7	74.6 ± 5.5	60.3 ± 7.5	75.3 ± 5.7

Values are means ± SD or *n* (%). COPD, chronic obstructive pulmonary disease; FEV1, forced expiratory volume in one second; FVC, forced vital capacity; GEO, Gene Expression Omnibus.

demographics were previously reported (25) and presented in Table 3.

Cell Culture and Transfections

The human airway epithelial cell line, 1HAEo, was obtained from Dr. Dieter Gruenert (UCSF) (26) and cultured in DMEM (Invitrogen) with 10% fetal bovine serum (FBS; ThermoFisher 12483020) and 1% penicillin-streptomycin (ThermoFisher 15140122). For all procedures, the media and applicable supplements were replaced every 2 days.

For gene knockout with CRISPR-Cas9, 5′-AGCAGGATGAAGTTCGACAT-3′ (IDT), which corresponded to a unique guide RNA targeting, an early canonical gene exon of human *FAM13A*, was cloned into BbsI-digested pX458 (Addgene 48138) to yield pX458-hFAM13A-4.2. Following sequence confirmation, this clone was propagated in DH5α *E. coli* (27). Guide sequences were chosen based on high-quality scores, and minimal off-target sites and mismatches according to crispr.mit.edu. DNA plasmids were transfected into 1HAEo cells using lipofectamine 3000 (Invitrogen) for 24 h according to the manufacturer's protocol. Cells positive for Cas9-GFP expression were single cell-sorted by flow cytometry into 96-well plates and maintained in complete media until colonies were formed. The expanded clones were secondarily screened for FAM13A knockdown using Western blots, and candidate null clones were confirmed by PCR sequencing of the targeted genomic loci covering the PAM motif. For experiments, wild-type (WT) and *FAM13A*$^{-/-}$ cells were cultured in reduced serum (1% FBS) and treated with 10 ng/mL TGF-β1 for 7 days (28, 29).

For gene silencing with RNAi using lipofectamine 3000 (L3000015; Thermo Fisher Scientific), cells were cultured in 1% FBS and pretreated with 25 nM silencer-select scrambled or CTNNB1 siRNA (ThermoFisher 4390843 or s19753) for 2 days, followed by another round of siRNA treatment in the presence or absence of 10 ng/mL TGF-β1 (BioLegend 580704) for 5 days.

For the intervention study, 1HAEo cells were cultured in 1% FBS and pretreated with 100 ng/mL PKF118-310 (inhibits TCF4/CTNNB1 complex) (K4394; Sigma) for 2 days, followed by PKF118-310 in the presence or absence of 10 ng/mL TGF-β1 (BioLegend 580704) for 5 days.

Real-Time PCR

PCR methods and analysis have been previously described (30). In brief, human TaqMan probes (Life Technologies) were used to measure expression of *FAM13A* (Hs00208453_m1), *COL1A1* (Hs00164004_m1), *MMP2* (Hs01548727_m1), and *CDH1* (Hs01023894_m1) and *CTNNB1* (Hs99999168_m1) with normalization to *GAPDH* (Hs02758991_g1). Gene expression was expressed as ΔCt (relative quantitation) and ΔΔCt (fold changes) with normalization to control values.

Western Blot

Western blot methods and analysis have been previously described (30, 31). In brief, 25 μg of whole cell lysate extracted using cell lysis buffer (Cell Signaling 9803) or nuclear/cytoplasmic lysate extracted using the NE-PER Nuclear and Cytoplasmic Extraction Reagents (ThermoFisher 78833) was resolved by 10% SDS-PAGE, and transferred to nitrocellulose (Biorad 1704159) using the Trans-Blot Turbo Transfer System (Biorad 17001917). Membranes were incubated with primary antibodies against FAM13A (Sigma HPA038109), COL1A1 (Abcam Ab34710), total CTNNB1 (Cell Signaling 9562S), active CTNNB1 (Cell Signaling 8814S), MMP2 (Cell Signaling 40994), CDH1 (Abcam ab40772), β-actin (Sigma A1978), and histone deacetylase 2 (HDAC2) (Cell Signaling 5113S), followed by incubation with IRDye anti-rabbit and/or anti-mouse IgG secondary antibodies (Li-Cor 926–68071 and 926–32210) and visualized using Odyssey CLx (LI-COR Biosciences).

Immunofluorescence Staining and Confocal Microscopy

To visualize COL1A1 and CTNNB1 protein expression, cells were fixed with formalin, permeabilized by Triton X, and incubated with primary antibodies against COL1A1 (Cell Signaling 39952) and total CTNNB1 (Cell Signaling 9562S) overnight at 4°C, and stained with Alexa Fluor- 488 goat anti-mouse IgG and 594 goat anti-rabbit IgG (Life Technologies) for 2 h at room temperature. To visualize the effect of TGF-β1 on filamentous actin (F-actin) organization, WT and *FAM13A*$^{-/-}$ cells were fixed and stained with fluorescein-phalloidin (ThermoFisher F432) as per the manufacturer's instruction. Slides were counterstained with DAPI for cell nuclei (Sigma 10236276001), cover-slipped and visualized using confocal microscopy at ×20 magnification. Fluorescence intensity from the entire image was normalized to nuclei count using ImageJ.

Preparation of Lipid Nanoparticles

Lipid nanoparticles (LNPs) composed of ionizable lipid/phosphatidylcholine/cholesterol/PEG-lipid (50/10/38.5/1.5 mol %) were prepared using rapid-mixing techniques (32–34). Lipid components dissolved in ethanol (10 mM total lipid) were combined with 25 mM sodium acetate pH 4 and dialyzed into the same buffer to remove solvent. The resulting preformed vesicles were concentrated and stored until use in transfections. Using a benchtop-mixing procedure described elsewhere (35), we combined mRNA with LNP at a ratio of 29 μg RNA per μmol lipid immediately before dilution into cell media.

Lipofectamine and LNP-Mediated Delivery of *GFP* and *FAM13A* mRNA

First, LNP-mRNA uptake efficiency was evaluated by incorporation of the nonexchangeable lipid dye 1,1-dioctadecyl-3,3,3,3-tetramethylindodicarbocyanine (DiD) at 0.2 mol%. Second, to validate the transfection efficiency of the developed LNP system, CleanCap *eGFP* mRNA (L-7201; Trilink Biotech) was encapsulated and used for transfection of 1HAEo cells at a final concentration of 3 μg mRNA/mL for 24 h. Lipofectamine 3000 was used as a positive control for the transfection of *eGFP* mRNA. To overexpress FAM13A, the coding sequence of the human *FAM13A* mRNA, transcript variant 2 (NM_001015045.2) was obtained from Trilink BioTechnologies (L-7007) and encapsulated into LNPs as described. Cells were treated with TGF-β1 for 3 days, followed by a refreshment of TGF-β1 + LNPs entrapping *FAM13A* mRNA at 1 or 3 μg mRNA/mL for 4 days. To model a more acute induction of total and active CTNNB1 in both cytoplasmic and nuclear fractions, cells were treated with TGF-β1 for 1 day, followed by a refreshment of TGF-β1 + LNPs entrapping *FAM13A* mRNA at 3 μg mRNA/mL for 3 days. RNA and protein were extracted for real-time PCR and Western blot analyses, respectively.

Flow Cytometry Analysis

To assess the percentages of GFP + cells, 1HAEo cells were analyzed by flow cytometry (Gallios, Beckman Coulter). Briefly, cells were lifted with trypsin (Invitrogen 25200056) for 2 min at 37°C followed by neutralization with 10% FBS-DMEM, fixed with 10% formalin for 10 min, and resuspended in 2% FBS-PBS. Kaluza for Gallios acquisition software (Beckman Coulter) was used to analyze the percentage of GFP + and DiD + cells in the samples.

Cell Imaging

To observe single-cell dynamics in real time, cells were seeded at low density in 10% FBS-DMEM and allowed to attach for 5 h. Fresh complete media was replaced before live cell imaging every min for 3 h. To observe changes in cellular morphology relative to density over time, WT and *FAM13A*$^{-/-}$ 1HAEo cells were seeded at low density in 10% FBS-DMEM with fresh complete media containing TGF-β1 replaced every 2 days.

Statistical Methods

In vitro and ex vivo study data were tested for normality before the selection of a parametric (normal distribution) or Mann–Whitney (non-normal distribution) *t* test, Kruskal–Wallis multiple comparisons test, one-way ANOVA with Bonferroni's multiple comparisons test, and linear regression test, where appropriate. All data were analyzed using GraphPad Prism 8 (GraphPad Software Inc.) and were expressed as means ± SE. Statistical significance was considered at $P < 0.05$.

RESULTS

Expression of FAM13A Is Increased and CTNNB1 Is Decreased in the Airway Epithelium of Patients with COPD

To determine the relationship between FAM13A and CTNNB1 expression in airway epithelium, FAM13A expression in lung tissue samples from nonsmoking controls and subjects with COPD was evaluated by immunohistochemistry. The demographics of this cohort is shown in Table 1. Representative images of airway epithelial-specific FAM13A protein expression in nonsmoking controls and patients with COPD with GOLD 2 and GOLD 4 are shown in Fig. 1, *A–C*. FAM13A expression was significantly increased in the airway epithelia of patients with moderate to severe COPD (as defined by GOLD stages 3 and 4) when compared with those from nonsmoking controls (Fig. 1*D*). After stratification of patients with COPD by smoking status, epithelial-specific FAM13A expression was highest in current smokers when compared with nonsmoking controls and moderately elevated in ex-smokers (Fig. 1*E*). Interestingly, we observed a significant negative correlation between the epithelial-specific FAM13A expression and forced expiratory volume in one second (FEV1) to vital capacity (FVC) percent predicted (%) (Fig. 1*F*), indicating that FAM13A expression is increased with decreasing lung function. To determine the expression of several key regulatory genes associated with the TGF-β1 signaling pathway in human airway epithelial cells, gene expression data set were assessed in healthy nonsmokers (n = 68 subjects), smokers without COPD (n = 101), and smokers with COPD (n = 42; Table 2). *TGFβ1* and *COL1A1* gene expressions were upregulated, whereas *CDH1* and *CTNNB1* were downregulated in the airway epithelium of smokers with COPD compared with healthy nonsmokers (Fig. 1*G*). *FAM13A* expression was positively associated with *CTNNB1* and negatively associated with *COL1A1* expression (P = 3.79E-06; P = 1.43E-09, respectively) (Fig. 1, *H–I*).

In a replication cohort (Table 3), current smokers exhibited decreased *CTNNB1* expression compared with ex-smokers, irrespective of COPD status (P = 0.002132; Supplemental Fig. S1*A*; see https://doi.org/10.6084/m9.figshare.14036300). After adjustment for age, sex, and smoking status, subjects with COPD had decreased *CTNNB1* expression compared with subjects without COPD (P = 0.0000867) (Supplemental Fig. S1*B*). After adjustment for age, sex, and smoking status, prebronchodilator FEV1 and FEV1/FVC were positively associated with expression of *CTNNB1* (P = 0.00087; P = 0.00039, respectively, Supplemental Fig. S1, *C* and *D*). Consistent with the cohort in Table 2, *FAM13A* expression was positively associated with *CTNNB1* and negatively associated with *COL1A1* expression (P = 0.0091; P = 0.000014, respectively, Supplemental Fig. S1, *E* and *F*). Collectively, these data provide clinical confirmation on the positive association of *FAM13A* with *CTNNB1*, and the negative association of *FAM13A* with *COL1A1*, in the airway epithelium of subjects with or without COPD.

FAM13A$^{-/-}$ Cells Exhibit Increased COL1A1 and MMP2 Expression in Response to TGF-β1

To determine the biological role of FAM13A in response to TGF-β1 stimulation, we used CRISPR-Cas9 gene editing (27) to negate FAM13A expression (*FAM13A*$^{-/-}$) in 1HAEo cells. Sequencing of the targeted *FAM13A* genomic loci revealed indel frameshift mutations resulting in premature translational termination, with loss of FAM13A protein expression confirmed by a Western blot analysis (Fig. 2, *A–C*). Representative immunofluorescence images and quantitation showed

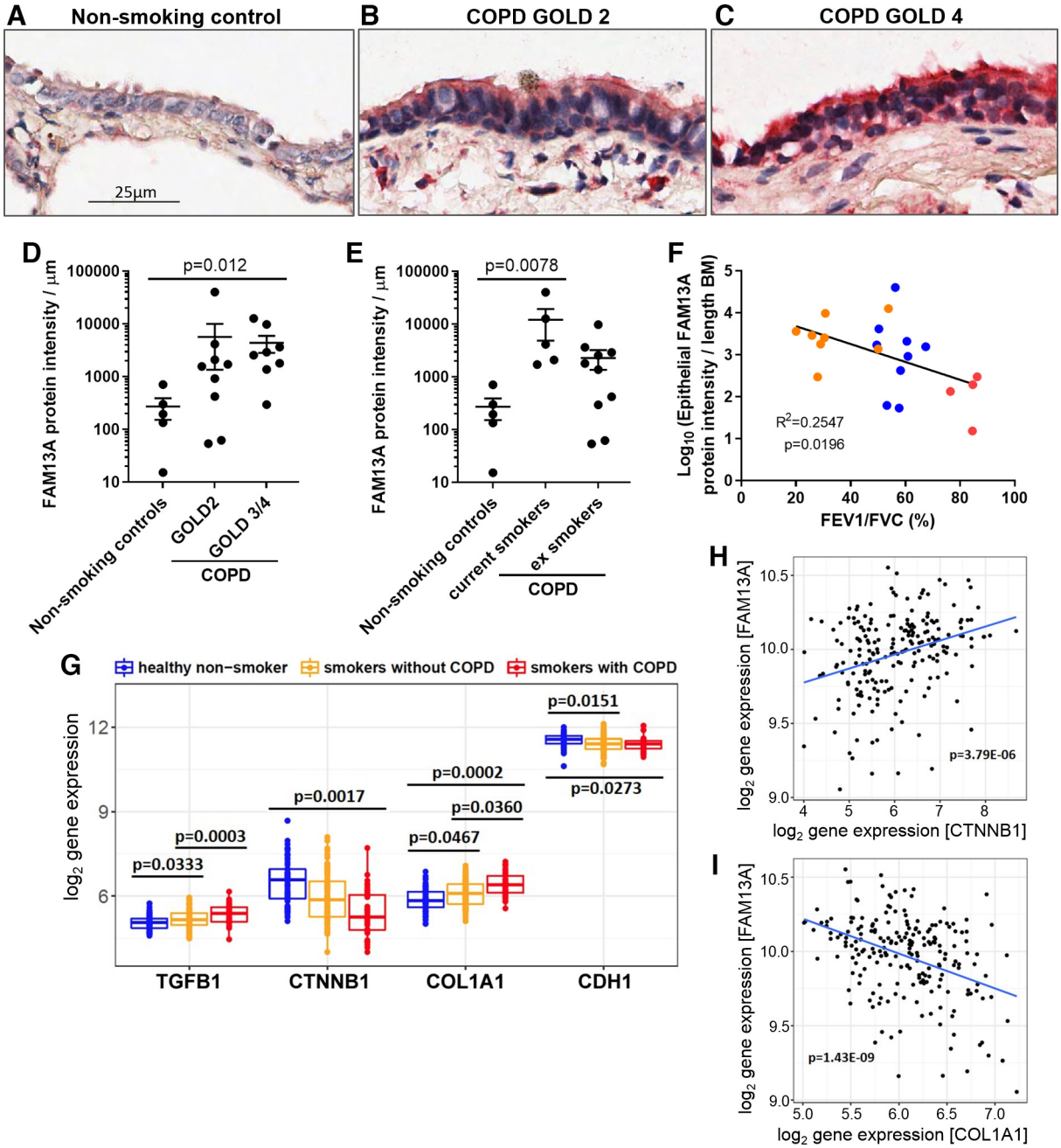

Figure 1. FAM13A protein expression is upregulated in the airway epithelium of patients with COPD. Representative images of paraffin-embedded human lung tissues from nonsmoking control (*A*), COPD GOLD 2 (*B*), and COPD GOLD 4 (*C*) stained for FAM13A protein expression. *D*: airway-specific FAM13A expression was quantified and normalized to length of basement membrane in micrometer. *E*: airway-specific FAM13A expression was stratified by smoking status in patients with COPD (current vs. ex-smokers). *F*: correlation between total epithelial-specific FAM13A expression (data log-transformed) with FEV1/FVC (%). Values were expressed as means ± SE. The Kruskal–Wallis test with Dunnett's multiple comparisons test was used in *D* and *E*. (Note: one non-COPD subject has no reported FEV1/FVC ratio in *F*). In *F*, red dots = nonsmoking controls, blue dots = COPD GOLD2, and orange dots = COPD GOLD 3, 4. *G*: boxplots of *TGFβ1*, *CTNNB1*, *COL1A1*, and *CDH1* gene expression in the small airway epithelium of ($n = 68$) healthy nonsmokers, ($n = 101$) smokers without COPD, and ($n = 42$) smokers with COPD (box indicates the median and the interquartile range). Gene expression correlation analyses between *CTNNB1* and *FAM13A* (*H*), and *COL1A1* and *FAM13A* (*I*). The *P* value was obtained using a linear regression model with gene expression as the response variable and adjusted for age, sex, and smoking status. CDH1, E-cadherin; COL1A1, collagen type 1; COPD, chronic obstructive pulmonary disease; CTNNB1, β-catenin; FAM13A, Family with sequence similarity 13, member A; FEV1, forced expiratory volume in one second; FVC, forced vital capacity; GOLD, global initiative for chronic obstructive lung disease.

an increase in COL1A1 protein expression in TGF-β1-treated *FAM13A*$^{-/-}$ cells when compared with the WT counterpart (Fig. 3, *A* and *B*). Real-time PCR analyses consistently showed that *FAM13A*$^{-/-}$ cells mounted a greater induction in TGF-β1-mediated increase in *COL1A1* gene expression compared with WT cells (Fig. 3*C*). Similarly, *FAM13A*$^{-/-}$ cells exhibited increased *MMP2* gene expression when compared with WT cells, and this increase was further elevated in response to

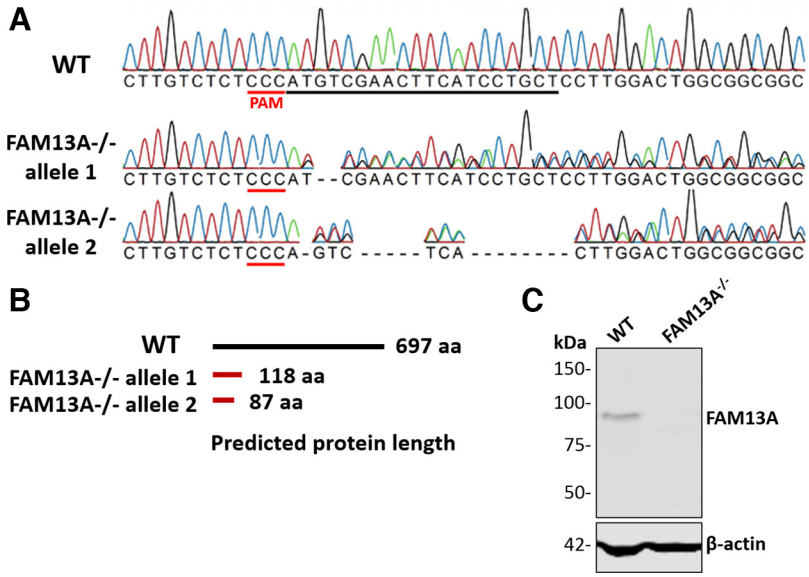

Figure 2. Generation of *FAM13A*$^{-/-}$ 1HAEo cells using CRISPR-Cas9. *A*: sequencing of the *FAM13A* genomic loci of WT 1HAEo cells and a *FAM13A*$^{-/-}$ clone generated using CRISPR-Cas9 targeting. Targeted guide RNA sequence indicated with black line; PAM recognition motif indicated with red. Alignment indicated a 2-bp deletion in one allele and a net 14-bp deletion in the other allele. *B*: both frame-shifted alleles encode for predicted truncated proteins of 118 and 87 amino acids resulting from premature termination codons. Wild-type FAM13A is 697 amino acids long. *C*: Western blot analysis for FAM13A and β-actin expression of lysates from 1HAEo WT and *FAM13A*$^{-/-}$ cells. FAM13A, Family with sequence similarity 13, member A; 1HAEo, human airway epithelial cell line; WT, wild-type.

TGF-β1 treatment (Fig. 4*A*). The increases in *MMP2* transcripts correlated well to increases in MMP2 protein expression as detected by Western blot analyses (Fig. 4, *B* and *C*). Taken together, these data showed that the loss of FAM13A expression in human airway epithelial cells enhances the transcriptional regulation of COL1A1 and MMP2 expression after TGF-β1 activation.

Active CTNNB1 Expression Is Elevated in *FAM13A*$^{-/-}$ Cells and Further Induced by TGF-β1

Previously, it was reported that a loss of FAM13A increases the stability and expression of CTNNB1, which protects mice from chronic smoke-induced emphysema (19). Since CTNNB1 is also a transcriptional coregulator that is involved in EMT (36), we determined whether FAM13A regulation of EMT genes such as *COL1A1* and *MMP2* occurs via modulation of CTNNB1. Expression of total CTNNB1 was upregulated in *FAM13A*$^{-/-}$ cells compared with WT, whereas stimulation with TGF-β1 further elevated the levels of CTNNB1 in *FAM13A*$^{-/-}$ cells (Fig. 5, *A* and *B*). In addition, active CTNNB1 levels were also upregulated in *FAM13A*$^{-/-}$ cells when compared with WT cells after TGF-β1 treatment (Fig. 5, *C* and *D*). When visualized by immunofluorescence imaging, total CTNNB1 expression localized in the cytoplasmic and plasma membrane compartments was increased in *FAM13A*$^{-/-}$ cells when compared with WT, which was further elevated upon treatment with TGF-β1 (Fig. 5*E*). Western blot quantification of cytoplasmic and nuclear fractions revealed a consistent increase in total and active CTNNB1 protein in *FAM13A*$^{-/-}$ cells treated with TGF-β1, but not in WT cells (Fig. 5, *F–I*). These data showed that a loss of FAM13A increases total and active CTNNB1 expression after TGF-β1 treatment.

Inhibition of CTNNB1 Reduces TGF-β1-Induced Increase in COL1A1 and MMP2 Expression

To demonstrate the potential contribution of CTNNB1 in mediating TGF-β1-induced increase in COL1A1 and MMP2 expression, cells were pretreated with CTNNB1 siRNA or with PKF118-310, a small molecule antagonist of the TCF4/CTNNB1 signaling complex (37), followed by 5 days of TGF-β1 treatment. CTNNB1 gene and protein expression were significantly reduced in *CTNNB1* siRNA-treated groups compared with scrambled siRNA-treated groups in WT cells (Supplemental Fig. S2, *A–C*; see https://doi.org/10.6084/m9.figshare.13058954). Treatment of WT cells with CTNNB1 siRNA reduced TGF-β1-induced increase in COL1A1 and MMP2 gene and protein expression (Fig. 6, *A–D*). Similarly, pharmacological inhibition of TCF4/CTNNB1 complex using PKF118-310 reduced TGF-β1-induced increase in COL1A1 gene and protein expression (Fig. 6, *E* and *F*). PKF118-310 reduced TGF-β1-induced increase in MMP2 protein but not gene expression (Fig. 6, *G* and *H*). Next, to determine whether silencing CTNNB1 with siRNA impacts COL1A1 in *FAM13A*$^{-/-}$ cells, we first confirmed that CTNNB1 siRNA treatment reduced CTNNB1 protein expression to below control levels in the presence or absence of TGF-β1, and recapitulated the induction of CTNNB1 protein by TGF-β1, but did not modify COL1A1 expression (Supplemental Fig. S2, *D–G*). Collectively, these data showed that CTNNB1 is partially required in TGF-β1-induced increase in the expression of COL1A1 and MMP2.

FAM13A Overexpression Reduces TGF-β1-Induced Increase in COL1A1 and MMP2 Expression

Given that reduced FAM13A expression led to upregulation of COL1A1 and MMP2 expression via TGF-β1, we determined whether the overexpression of FAM13A reverses this phenomenon. Initially, we used lipofectamine to transfect cells with *FAM13A* mRNA, and showed that *FAM13A* overexpression attenuated TGF-β1-induced increase in *COL1A1* but not *MMP2* gene expression (Supplemental Fig. S3, *A–C*; see https://doi.org/10.6084/m9.figshare.13058960). Due to its inherent toxicity and its ability for immune activation, lipofectamine has little clinical utility. Therefore, we next evaluated the therapeutic potential of *FAM13A* overexpression using clinically validated LNP technology (38, 39). We encapsulated mRNA in LNP for cellular overexpression. Using flow cytometry to assess GFP + cells as an indicator of

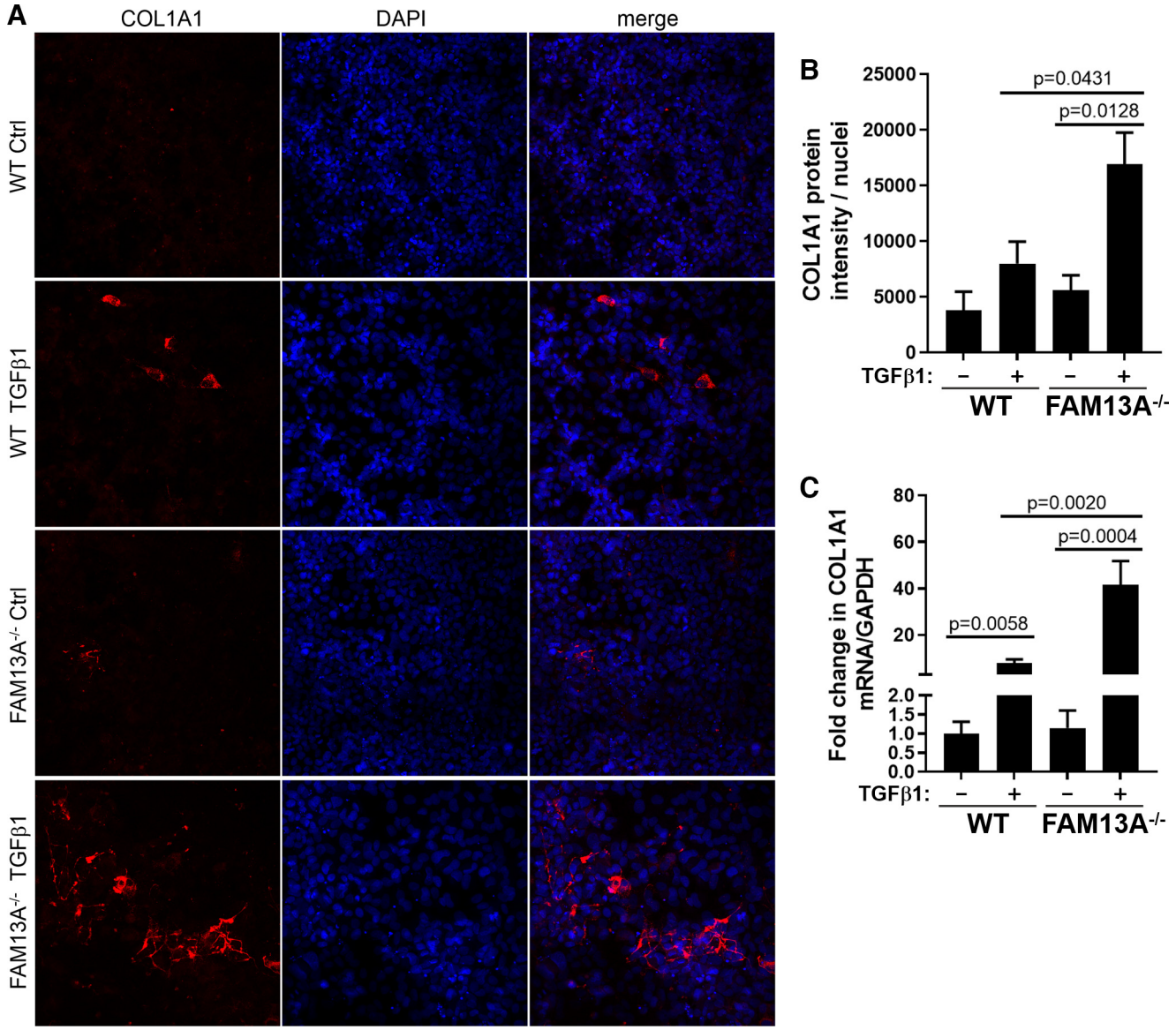

Figure 3. Loss of FAM13A promotes increased COL1A1 protein expression in response to TGF-β1 stimulation. *A*: representative confocal images of COL1A1 protein expression, with DAPI counterstaining for nuclei, in WT and *FAM13A*$^{-/-}$ cells with and without TGF-β1 treatment (1 wk). Scale bar = 100 μm. *B*: assessment of COL1A1 protein intensity normalized to number of nuclei. *C*: gene expression of *COL1A1* normalized to *GAPDH* in WT and *FAM13A*$^{-/-}$ cells at baseline were expressed as fold change normalized to WT controls. Values were expressed as means ± SE ($n = 4$ independent experiments). One-way analysis of variance with Bonferroni's multiple comparisons test was used in *B* and *C*. COL1A1, collagen type 1; FAM13A, Family with sequence similarity 13, member A; WT, wild-type.

transection efficiency, we found that lipofectamine and LNP-based transfection resulted in comparable levels of efficiency (79.8% and 84.8% GFP+, respectively) when compared with untreated or *GFP* mRNA only controls (Supplemental Fig. S4, *A*–*E*; see https://doi.org/10.6084/m9.figshare.13058963). In addition, LNP uptake into cells was 100% as indicated by DiD-colabeling (Supplemental Fig. S4*F*).

As expected, FAM13A gene and protein expression was increased in cells treated with LNP-encapsulated *FAM13A* mRNA (Supplemental Fig. S5, *A* and *B*; see https://doi.org/10.6084/m9.figshare.14385302). LNP-mediated transfection of cells with *FAM13A* mRNA led to reduced TGF-β1-induced increase in COL1A1 and MMP2 gene and protein expression (Fig. 7, *A*–*D*). TGF-β1 treatment significantly reduced both CDH1 gene and protein expression, this reduction was not further modified for cells transfected with *FAM13A* mRNA (Fig. 7, *E* and *F*). Total CTNNB1 protein expression was significantly reduced in cells treated with *FAM13A* mRNA when compared with untreated controls (Fig. 7*G*). The combination of *FAM13A* mRNA and TGF-β1 treatment led to significant reduction of active CTNNB1 protein expression when compared with untreated controls (Fig. 7*H*). Finally, we analyzed total and active CTNNB1 in cytoplasmic and nuclear fractions of 1HAEo cells treated with combinations of FAM13A and TGF-β1 for 3 days. *FAM13A* mRNA consistently prevented TGF-β1-induced increases in total and active cytoplasmic CTNNB1 (Fig. 7, *I* and *J*), as well as total nuclear

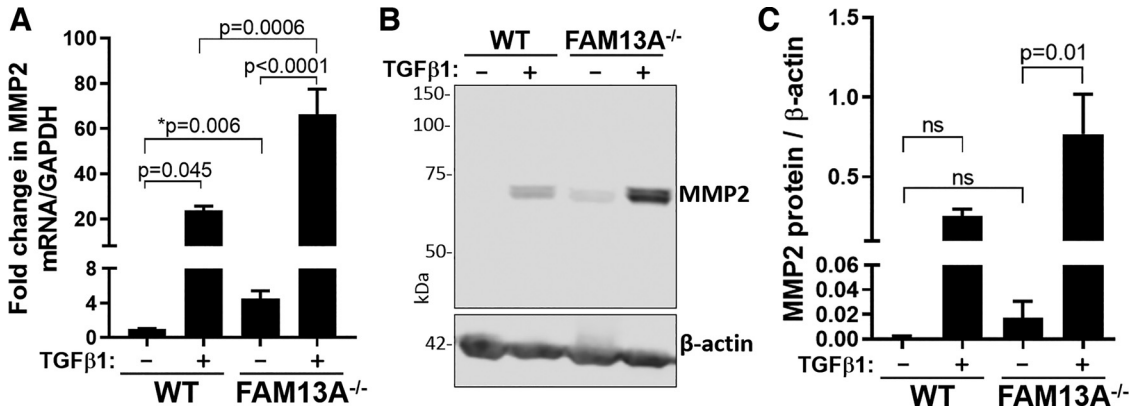

Figure 4. Loss of FAM13A promotes increased MMP2 expression in response to TGF-β1 stimulation. *A*: assessment of fold change in expression of *MMP2* normalized to *GAPDH* in WT and *FAM13A*$^{-/-}$ cells in the absence or presence of TGF-β1 treatment (1 wk). *B*: representative Western blot. *C*: quantification of MMP2 protein expression normalized to β-actin in WT and *FAM13A*$^{-/-}$ cells in the absence or presence of TGF-β1 treatment. Values were expressed as means ± SE ($n = 4$ independent experiments). One-way analysis of variance with Bonferroni's multiple comparisons test was used in *A* and *C*. FAM13A, Family with sequence similarity 13, member A; MMP2, matrix metalloproteinase 2; WT, wild-type.

CTNNB1 (Fig. 7*K*), but not active nuclear CTNNB1 (Fig. 7*L*). In summary, *FAM13A* overexpression attenuated TGF-β1-induced increase in the expression of COL1A1 and MMP2, concomitant with reduced expression of total and active CTNNB1.

FAM13A Influences Cell Morphology and Skeletal Organization of F-actin

We compared the morphology of WT and *FAM13A*$^{-/-}$ cells transitioning from low-to-high density culture (Supplemental Fig. S6, *A*–*D*; see https://doi.org/10.6084/m9.figshare.13058966). Although both cells retained an overall epithelial-like morphology, *FAM13A*$^{-/-}$ cells exhibited greater spreading compared with WT cells. Treatment with TGF-β1 induced both WT and *FAM13A*$^{-/-}$ cells to adopt elongated shapes at low density, whereas at high density, cells appeared to be less densely packed with enhanced spreading compared with nontreated cells. Higher-resolution temporal imaging of non-TGF-β1-treated cells revealed lamellipodial protrusive activity that was enhanced in *FAM13A*$^{-/-}$ cells when compared with WT (Supplemental Video S1; see https://doi.org/10.6084/m9.figshare.14036318). Cytoskeletal remodeling is associated with EMT (40), thus cells were stained with phalloidin to visualize filamentous actin (F-actin). At higher cell densities, cortical F-actin indicative of cell-cell contact was evident in both WT and *FAM13A*$^{-/-}$ cells (Fig. 8*A*). *FAM13A*$^{-/-}$ cells treated with TGF-β1 resulted in reorganized F-actin that appeared less cortical and more like stress fibers (Fig. 8*A*). This phenomenon was also observed in TGF-β1-treated WT cells, albeit at attenuated levels. After normalization to nuclei counts, the overall F-actin staining intensity was increased in *FAM13A*$^{-/-}$ but not in WT cells after TGF-β1 stimulation (Fig. 8*B*). Cell packing density, assessed as number of nuclei per unit area at full cellular confluency, was intrinsically lower in *FAM13A*$^{-/-}$ compared with WT cells at baseline, and this effect was consistently decreased in both WT and *FAM13A*$^{-/-}$ cells after TGF-β1 treatment (Fig. 8*C*). Taken together, FAM13A is involved in cytoskeletal organization of F-actin, and TGF-β1-induced changes in COL1A1 and MMP2 expression and cell packing density.

DISCUSSION

In this study, we provide new data based on functional knockout of FAM13A expression in a human lung epithelial cell model designed to assess the role of FAM13A in response to TGF-β1 stimulation, which highlights a negative causal relationship between FAM13A and CTNNB1 expression in airway epithelial cells. Specifically, we showed that a complete loss of FAM13A expression in lung epithelial cells enhances TGF-β1's ability to increase the expression of COL1A1 and MMP2 by upregulating CTNNB1 expression, whereas overexpression of *FAM13A* attenuated the expression of COL1A1, MMP2, and CTNNB1. In analyses of airway epithelial cells from human subjects, we found that FAM13A protein expression was upregulated, whereas *CTNNB1* gene expression was downregulated in smokers with COPD than in healthy nonsmokers. Collectively, these data suggest that FAM13A is a modifier of TGF-β1-mediated signaling and its upregulation in smokers at risk for COPD may protect the lungs against epithelial remodeling that leads to progressive narrowing of the airways in COPD.

Mass spectrometry studies of FAM13A-interacting proteins have implicated pathways enriched in "CTNNB1 phosphorylation cascade" and "CTNNB1 degradation by the destruction complex" (19). The proposed canonical mechanism by which TGF-β1 regulates extracellular matrix-related gene expression is through phosphorylation of Smad2/3, and their subsequent translocation to the nucleus to regulate transcription (41). In connecting the role of CTNNB1 in TGF-β1 signaling, Zhou et al. (42) showed a direct interaction between Smad3 and CTNNB1 in the regulation of α-smooth muscle actin (αSMA) after TGF-β1 stimulation. It was also reported that siRNA-mediated silencing of CTNNB1 reduces TGF-β1-induced matrix production in airway smooth muscle cells (36). Growth factors such as TGF-β1 play a critical role in the pathogenesis of airway remodeling in COPD (43) and asthma (44). TGF-β1 is a multifunctional cytokine that is stored in the extracellular matrix compartment in its inactive form (45). Latent TGF-β1 can be activated via oxidation (46) or enzymatically cleaved to release the active form of TGF-β1 for the activation of structural and inflammatory

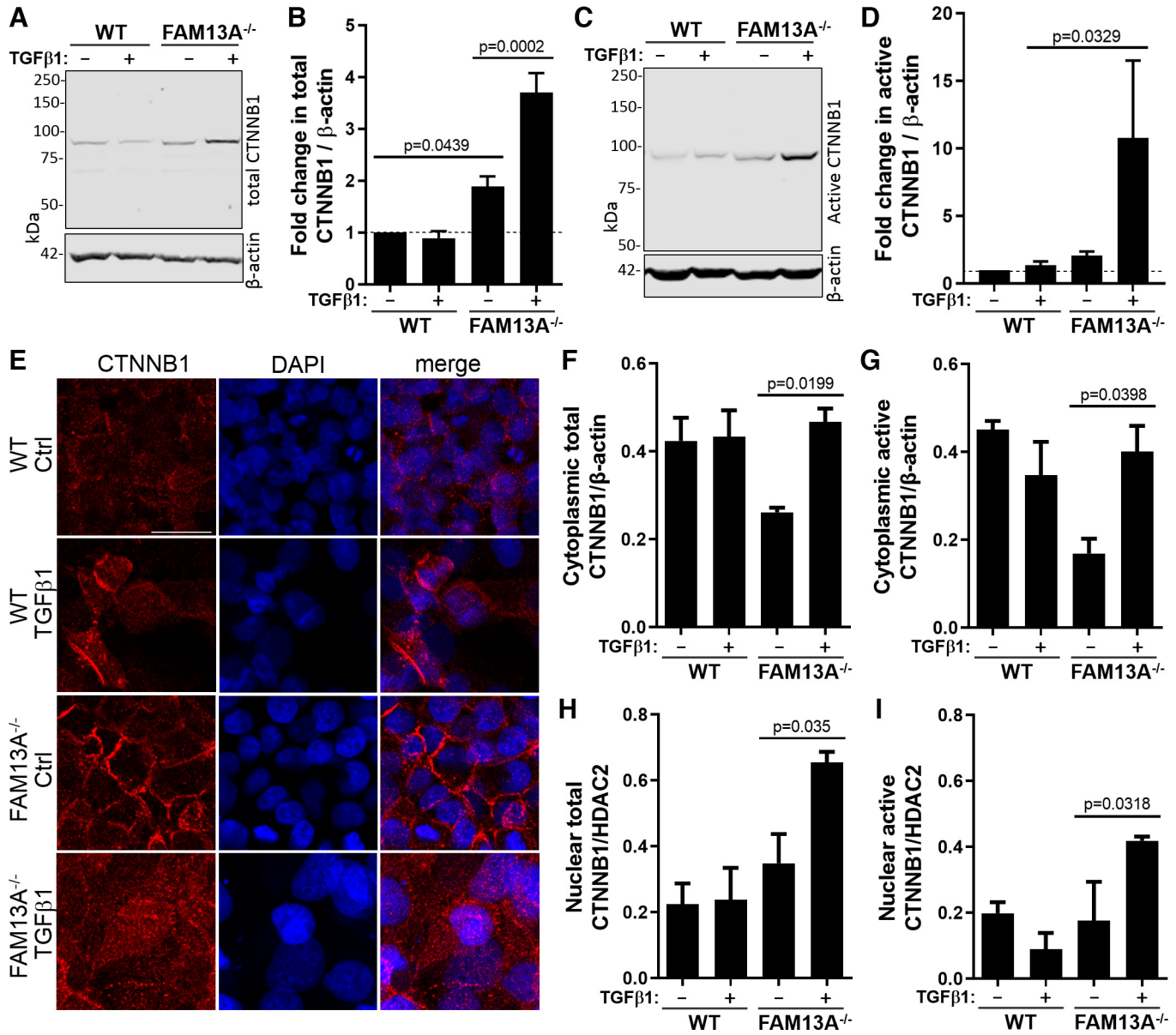

Figure 5. Loss of FAM13A promotes increased total and active CTNNB1 expression in response to TGF-β1 stimulation. *A*: representative Western blot and *B*: quantification of total CTNNB1 protein expression normalized to β-actin in WT and *FAM13A*$^{-/-}$ cells with and without TGF-β1 treatment. *C*: representative Western blot and *D*: quantification of active CTNNB1 protein expression normalized to β-actin in WT and *FAM13A*$^{-/-}$ cells with and without TGF-β1 treatment. *E*: representative confocal images of total CTNNB1 protein expression, with DAPI counterstaining for nuclei, in WT and *FAM13A*$^{-/-}$ cells with and without TGF-β1 treatment. Scale bar = 25 μm. Western blot quantification of total CTNNB1 (*F*) and active CTNNB1 cytoplasmic protein expression normalized to β-actin in WT and *FAM13A*$^{-/-}$ cells with and without TGF-β1 treatment (*G*). Western blot quantification of total CTNNB1 (*H*) and active CTNNB1 nuclear protein expression normalized to HDAC2 in WT and *FAM13A*$^{-/-}$ cells with and without TGF-β1 treatment (*I*). Values were expressed as means ± SE ($n = 3$ or 4 independent experiments). One-way analysis of variance with Bonferroni's multiple comparisons test was used in *B*, *D*, and *F*–*I*. CTNNB1, β-catenin; FAM13A, Family with sequence similarity 13, member A; WT, wild-type.

cells (47), thereby resulting in the production and secretion of extracellular matrix and tissue remodeling.

In search of novel therapeutic targets to reduce airway tissue remodeling, we turned to validating genes identified from COPD genome-wide association studies that are strongly associated with lung function with known biology. This is because the likelihood of success of such therapeutics in phase II clinical trials is 50%–100% greater compared with therapeutic targets that are disconnected from genetics (48–50). To determine the role of FAM13A and CTNNB1 in TGF-β1-induced EMT, we used CRISPR-Cas9 gene editing technology to generate 1HAEo cells deficient in both alleles of *FAM13A*. Corvol et al. (40) showed that FAM13A knockdown with siRNA augmented TGF-β1-induced αSMA and vimentin gene expression, and F-actin fiber formation in A549 cells. We extend these findings by showing that *FAM13A*$^{-/-}$ 1HAEo cells exhibited increased expression of COL1A1, MMP2, CTNNB1, and F-actin, molecules known to be involved in airway remodeling. It was reported that F-actin localizes at the margins of airway epithelial cells from nonsmokers, whereas

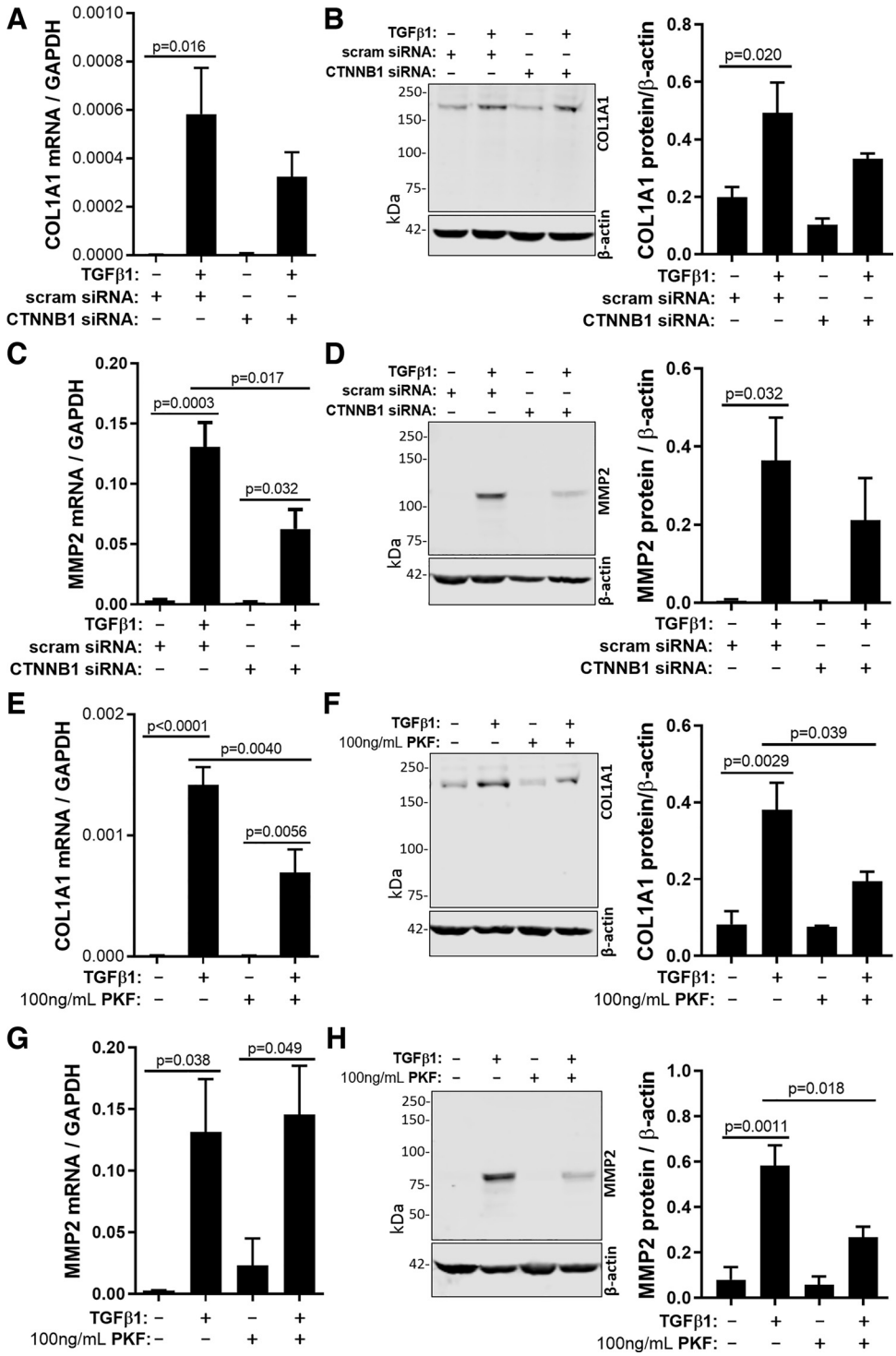

Figure 6. Effect of CTNNB1 siRNA and pharmacological inhibitor on TGF-β1-induced COL1A1 and MMP2 expression in 1HAEo cells. Wild-type 1HAEo cells were treated with control or CTNNB1 siRNA, in the absence or presence of TGF-β1 treatment, and assessed for (*A*) *COL1A1* gene expression relative to *GAPDH*, (*B*) COL1A1 protein expression relative to β-actin, (*C*) *MMP2* gene expression relative to *GAPDH*, and (*D*) MMP2 protein expression relative to β-actin. Wild-type 1HAEo cells were treated with control or 100 ng/mL PKF118-310, in the absence or presence of TGF-β1 treatment, and assessed for (*E*) *COL1A1* gene expression relative to *GAPDH*, (*F*) COL1A1 protein expression relative to β-actin, (*G*) *MMP2* gene expression relative to *GAPDH*, and (*H*) MMP2 protein expression relative to β-actin. As shown are representative Western blots and quantitation (*B*, *D*, *F*, *H*). Values were expressed as means ± SE ($n = 3$ independent experiments). One-way analysis of variance with Bonferroni's multiple comparisons test was used in all panels. COL1A1, collagen type 1; CTNNB1, β-catenin; 1HAEo, human airway epithelial cell line; MMP2, matrix metalloproteinase 2.

F-actin in cells from smokers and patients with COPD was distributed throughout the cytoplasm (18). In addition, TGF-β1 treatment of A549 cells also promoted the accumulation of cytoplasmic F-actin (51). Finally, to connect the regulatory role of CTNNB1, we showed that CTNNB1 siRNA treatment partially disrupted TGF-β1-induced increase in COL1A1 and MMP2 expression. Treatment with PKF118-310, an inhibitor of the interaction between T-cell factor 4 (Tcf4) and CTNNB1 complex, consistently reduced COL1A1 and MMP2 expression. Collectively, these data provide a more comprehensive understanding in the potential role of FAM13A in the regulation of CTNNB1 and in TGF-β1 signaling (52, 53), supporting an important implication in the context of airway tissue remodeling in patients at risk of developing severe COPD.

Single-nucleotide polymorphisms in *FAM13A* have previously shown a strong association with reduced lung function

and with increased risk of COPD; however, to date, its functional role in the pathogenesis of COPD has been unclear. Previously, Jiang et al. (19) reported an inverse relationship between FAM13A and CTNNB1 protein expression in human bronchial epithelial (16HBE) cell line, in mice studies and, in whole lung tissues from subjects with and without COPD. Our human tissue staining data specifically revealed an increase in FAM13A protein in the airway epithelium of

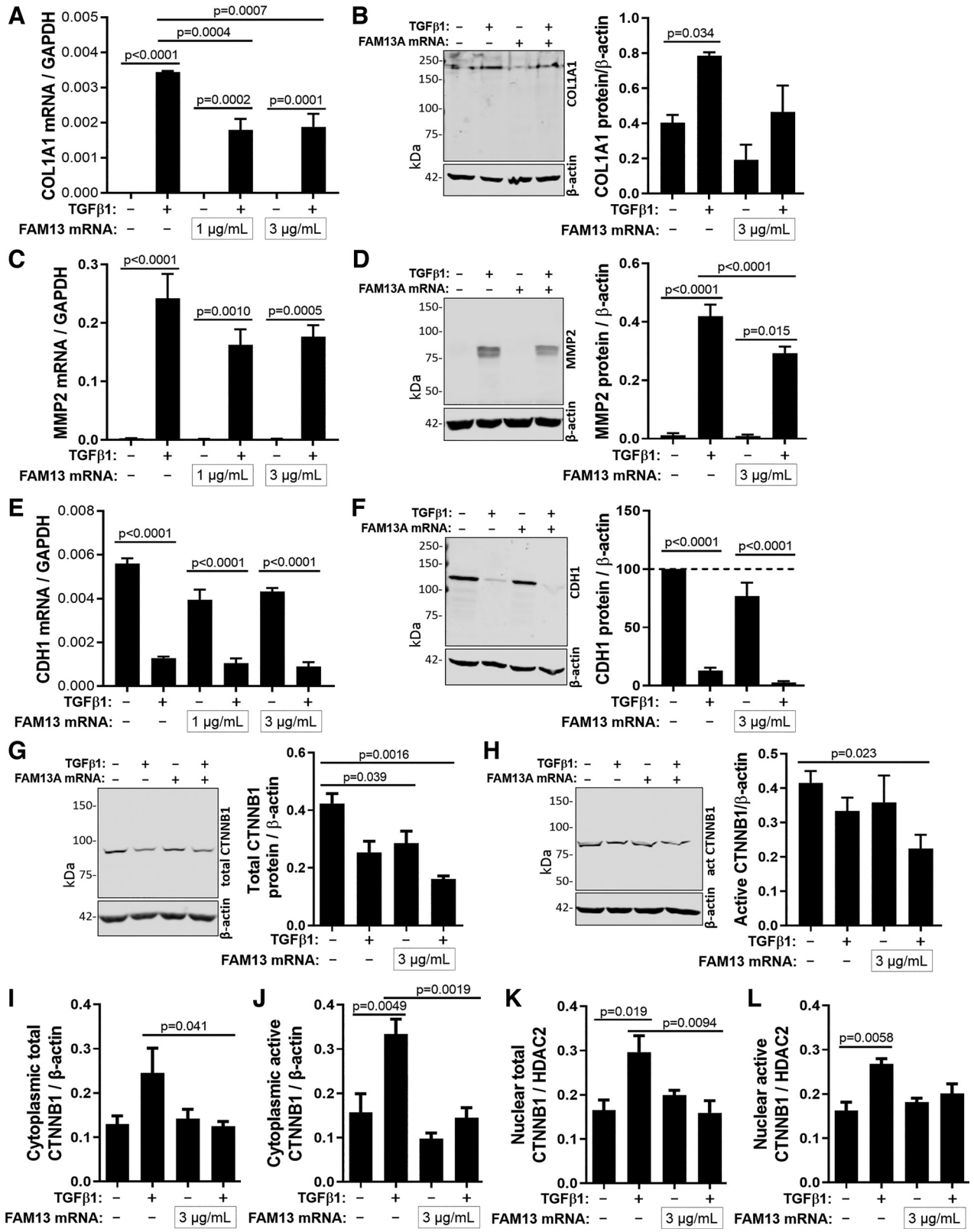

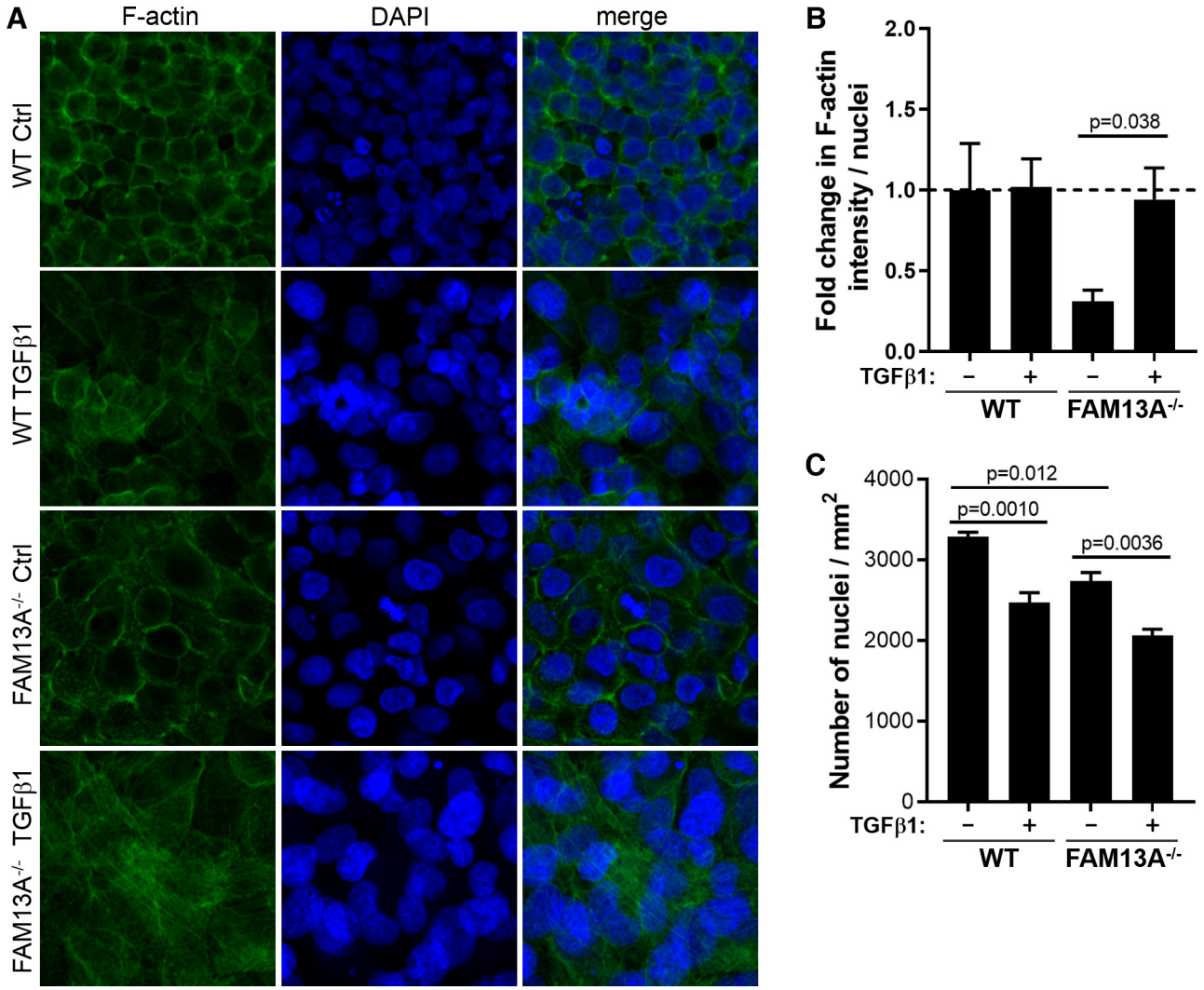

Figure 8. TGF-β1-induced remodeling of F-actin is enhanced in *FAM13A*$^{-/-}$ cells. *A*: representative confocal images and *B*: quantification of fold change in F-actin intensity/nuclei normalized to WT control were shown in WT and *FAM13A*$^{-/-}$ control cells in the presence or absence of TGF-β1 treatment. Scale bar = 25 μm. *C*: quantification on the number of nuclei per unit area was shown in WT and *FAM13A*$^{-/-}$ control cells at full confluency in the presence or absence of TGF-β1 treatment. Values were expressed as means ± SE ($n = 3$ independent experiments). A parametric *t* test was performed in *B*. One-way analysis of variance with Bonferroni's multiple comparisons test was used in *C*. FAM13A, Family with sequence similarity 13, member A; WT, wild-type.

patients with COPD compared with nonsmokers. Although it is tempting to speculate that FAM13A may play a role in enhancing airway tissue remodeling, our in vitro data indicates the contrary response, where FAM13A deficiency increased collagen expression via an increase in CTNNB1 upon stimulation with TGF-β1. This suggests that the increase in FAM13A expression observed in COPD airway epithelium may help to control excess TGF-β1-induced COL1A1 and MMP2 expression. The exact biological mechanism for the increase in FAM13A protein in COPD airway epithelium is unclear, but a previous study using an airway epithelial cell line showed that hypoxia increases FAM13A expression (54). Cigarette smoking is associated with increased risk of hypoxemia in patients with COPD (55, 56), which may partially explain the increase in FAM13A expression. Using lipid nanoparticle technology to encapsulate and deliver human *FAM13A* gene in 1HAEo cells, we showed that overexpression of *FAM13A* partially protects against TGF-β1-induced increase

Figure 7. LNP-mediated overexpression of *FAM13A* decreases TGF-β1-induced increase in COL1A1 and MMP2 expression in 1HAEo cells. Wild-type 1HAEo cells treated with empty LNP or LNP-*FAM13A* mRNA in the absence or presence of TGF-β1 treatment, and assessed for *COL1A1* gene expression relative to *GAPDH* (*A*), COL1A1 protein expression relative to β-actin (*B*), *MMP2* gene expression relative to *GAPDH* (*C*), MMP2 protein expression relative to β-actin (*D*), *CDH1* gene expression relative to *GAPDH* (*E*), CDH1 protein expression relative to β-actin (*F*), and total CTNNB1 (*G*), and active CTNNB1 protein expression relative to β-actin (*H*). Western blots shown are representative. 1HAEo cells treated with empty LNP or LNP-*FAM13A* mRNA in the absence or presence of TGF-β1 treatment (3 days), were also assessed for cytoplasmic total and active CTNNB1 relative to β-actin (*I* and *J*), and nuclear total and active CTNNB1 relative to β-actin (*K* and *L*). Values were expressed as means ± SE ($n = 3$ or 4 independent experiments). One-way analysis of variance with Bonferroni's multiple comparisons test was used in all panels. CDH1, E-cadherin; COL1A1, collagen type 1; CTNNB1, β-catenin; 1HAEo, human airway epithelial cell line; LNP, lipid nanoparticle; MMP2, matrix metalloproteinase 2.

in COL1A1 and MMP2 expression. Lipofectamine-mediated delivery of plasmids have commonly been used for cellular overexpression of genes of interests in cell culture models; however, net positive charges of lipofectamine-type agents have little clinical use owing to their increased toxicity (57), and the requirement to enter dividing cells for gene transcription. Lipid nanoparticles contain ionizable cationic lipids that bind to negatively charged RNA or DNA and form a protective coat that is net neutral at physiological pH. LNPs containing mRNA can directly release into the cytoplasm for immediate protein translation without integrating genetic information in our genome. Although DNA transfections are generally more stable than RNA transfections, RNA transfections present more diverse therapeutic options, as exemplified by adoption of the current RNA-based vaccines against COVID-19 (58, 59). Collectively, these data suggest that FAM13A overexpression maybe a potential strategy for therapeutic intervention in reducing airway tissue remodeling of smokers at risk for development of COPD.

In the present report, we use an in vitro model to demonstrate that a deficiency in FAM13A in response to TGF-β1 activates genes involved in airway tissue remodeling. Limitations not addressed by this model include an ideal confirmation for the role of FAM13A in airway epithelial remodeling in vivo that should be investigated using tissue-specific FAM13A KO generated in mice, and subjected to chronic cigarette smoke exposure. Furthermore, the contribution of other factors such as oxidative stress, local inflammatory response, and microbial interactions may synergistically enhance the TGF-β1 signaling response in the airway tissues of patients with COPD. The exact mechanism by which FAM13A is upregulated in the airway epithelium of patients with COPD is unknown and awaits resolution. However, we speculate that upregulation of FAM13A in the airway epithelium of healthy smokers without COPD may reduce CTNNB1 expression for a more protective response in controlling excess tissue remodeling. Undoubtedly, CTNNB1 (β-catenin) signaling contributes to lung repair/regeneration in response to various injuries (60, 61); therefore, more extensive studies accounting for multiple competing mechanisms at play are required to determine the value of overexpressing FAM13A in tissue-specific and disease-specific treatment.

In summary, this report shows that airway epithelial cells deficient in FAM13A loses its ability to sequester CTNNB1, and FAM13A is inversely related to the regulation of TGF-β1-mediated response in this in vitro model. Overexpression of FAM13A via LNP-mediated mRNA delivery partially reverses this effect in vitro. Moreover, the upregulation of FAM13A protein in the airway epithelium of patients at risk of COPD and those with mild COPD may offer increased protection against further TGF-β1-mediated tissue remodeling. This work provides important mechanistic insights in the role of FAM13A serving as a potential therapeutic target and limiting fibrotic response in the airway epithelium of smokers at risk of severe COPD by downregulating CTNNB1 that may intersect with TGF-β1-mediated tissue remodeling responses.

SUPPLEMENTAL DATA

Supplemental Fig. S1: https://doi.org/10.6084/m9.figshare.14036300.

Supplemental Fig. S2: https://doi.org/10.6084/m9.figshare.13058954.

Supplemental Fig. S3: https://doi.org/10.6084/m9.figshare.13058960.

Supplemental Fig. S4: https://doi.org/10.6084/m9.figshare.13058963.

Supplemental Fig. S5: https://doi.org/10.6084/m9.figshare.14385302.

Supplemental Fig. S6: https://doi.org/10.6084/m9.figshare.13058966.

Supplemental Video S1: https://doi.org/10.6084/m9.figshare.14036318.

ACKNOWLEDGMENTS

We thank Amrit Samra for processing the lung tissue samples for immunohistochemical staining, and Dean English for scanning the sections using the Aperio Imaging System.

GRANTS

A.T. is a recipient of a MITACS Accelerate fellowship award. P.R.C. acknowledges support from the Canadian Institutes of Health Research (CIHR FDN 148469) and the NanoMedicines Innovation Network (NMIN), a Canadian Networks of Centres of Excellence (NCE) in Nanomedicine. D.W. is supported by the Swiss National Science Foundation (No. 183923). J.A.K. is supported by the NMIN Postdoctoral Fellowship Award in Gene Therapy. D.D.S. is supported by the CIHR Grant 501100000024. This study receives support from the CIHR.

DISCLOSURES

P.R.C. has a financial interest in Acuitas Therapeutics and Precision NanoSystems. Acuitas is developing lipid nanoparticle (LNP) systems for therapeutic applications whereas Precision is developing apparatus to formulate LNPs. None of the other authors has any conflicts of interest, financial or otherwise, to disclose.

AUTHOR CONTRIBUTIONS

A.T., D.D.S., and C.J.L. conceived and designed research; A.T. performed experiments; A.T., P.L., C.X.Y., and X.L. analyzed data; A.T., X.L., D.W., and C.J.L. interpreted results of experiments; A.T., C.X.Y., and X.L. prepared figures; A.T. and C.J.L. drafted manuscript; A.T., P.L., L.V.L., C.X.Y., X.L., D.W., J.A.K., T-L.H., D.R.D., G.K.S., J.C.H., P.R.C., D.D.S., and C.J.L. edited and revised manuscript; A.T., P.L., L.V.L., C.X.Y., X.L., D.W., J.A.K., T-L.H., D.R.D. G.K.S., J.C.H., P.R.C., D.D.S., and C.J.L. approved final version of manuscript.

REFERENCES

1. **Agusti A**, **Hogg JC.** Update on the pathogenesis of chronic obstructive pulmonary disease. *N Engl J Med* 381: 1248–1256, 2019. doi:10.1056/NEJMra1900475.
2. **Celli BR**, **Wedzicha JA.** Update on clinical aspects of chronic obstructive pulmonary disease. *N Engl J Med* 381: 1257–1266, 2019. doi:10.1056/NEJMra1900500.
3. **Mittmann N**, **Kuramoto L**, **Seung SJ**, **Haddon JM**, **Bradley-Kennedy C**, **Fitzgerald JM.** The cost of moderate and severe COPD exacerbations to the Canadian healthcare system. *Respir Med* 102: 413–421, 2008. doi:10.1016/j.rmed.2007.10.010.
4. **Cho MH**, **McDonald ML**, **Zhou X**, **Mattheisen M**, **Castaldi PJ**, **Hersh CP**, **Demeo DL**, **Sylvia JS**, **Ziniti J**, **Laird NM**, **Lange C**, **Litonjua AA**, **Sparrow D**, **Casaburi R**, **Barr RG**, **Regan EA**, **Make BJ**, **Hokanson JE**, **Lutz S**, **Dudenkov TM**, **Farzadegan H**, **Hetmanski JB**, **Tal-Singer**

R, **Lomas DA**, **Bakke P**, **Gulsvik A**, **Crapo JD**, **Silverman EK**, **Beaty TH**; **NETT Genetics, ICGN, ECLIPSE and COPDGene Investigators.** Risk loci for chronic obstructive pulmonary disease: a genome-wide association study and meta-analysis. *Lancet Respir Med* 2: 214–225, 2014. doi:10.1016/S2213-2600(14)70002-5.

5. **Lamontagne M**, **Couture C**, **Postma DS**, **Timens W**, **Sin DD**, **Pare PD**, **Hogg JC**, **Nickle D**, **Laviolette M**, **Bosse Y.** Refining susceptibility loci of chronic obstructive pulmonary disease with lung eqtls. *PLoS One* 8: e70220, 2013. doi:10.1371/journal.pone.0070220.
6. **Lutz SM**, **Cho MH**, **Young K**, **Hersh CP**, **Castaldi PJ**, **McDonald ML**, **Regan E**, **Mattheisen M**, **DeMeo DL**, **Parker M**, **Foreman M**, **Make BJ**, **Jensen RL**, **Casaburi R**, **Lomas DA**, **Bhatt SP**, **Bakke P**, **Gulsvik A**, **Crapo JD**, **Beaty TH**, **Laird NM**, **Lange C**, **Hokanson JE**, **Silverman EK**; **ECLIPSE Investigators; COPDGene Investigators.** A genome-wide association study identifies risk loci for spirometric measures among smokers of European and African ancestry. *BMC Genet* 16: 138, 2015. doi:10.1186/s12863-015-0299-4.
7. **Obeidat M**, **Hao K**, **Bosse Y**, **Nickle DC**, **Nie Y**, **Postma DS**, et al. Molecular mechanisms underlying variations in lung function: a systems genetics analysis. *Lancet Respir Med* 3: 782–795, 2015. doi:10.1016/S2213-2600(15)00380-X.
8. **Pillai SG**, **Ge D**, **Zhu G**, **Kong X**, **Shianna KV**, **Need AC**, **Feng S**, **Hersh CP**, **Bakke P**, **Gulsvik A**, **Ruppert A**, **Lodrup Carlsen KC**, **Roses A**, **Anderson W**, **Rennard SI**, **Lomas DA**, **Silverman EK**, **Goldstein DB**; **ICGN Investigators.** A genome-wide association study in chronic obstructive pulmonary disease (COPD): identification of two major susceptibility loci. *PLoS Genet* 5: e1000421, 2009. doi:10.1371/journal.pgen.1000421.
9. **Siedlinski M**, **Tingley D**, **Lipman PJ**, **Cho MH**, **Litonjua AA**, **Sparrow D**, **Bakke P**, **Gulsvik A**, **Lomas DA**, **Anderson W**, **Kong X**, **Rennard SI**, **Beaty TH**, **Hokanson JE**, **Crapo JD**, **Lange C**, **Silverman EK**; **COPDGene and ECLIPSE Investigators.** Dissecting direct and indirect genetic effects on chronic obstructive pulmonary disease (COPD) susceptibility. *Hum Genet* 132: 431–441, 2013. doi:10.1007/s00439-012-1262-3.
10. **Cho MH**, **Boutaoui N**, **Klanderman BJ**, **Sylvia JS**, **Ziniti JP**, **Hersh CP**, **DeMeo DL**, **Hunninghake GM**, **Litonjua AA**, **Sparrow D**, **Lange C**, **Won S**, **Murphy JR**, **Beaty TH**, **Regan EA**, **Make BJ**, **Hokanson JE**, **Crapo JD**, **Kong X**, **Anderson WH**, **Tal-Singer R**, **Lomas DA**, **Bakke P**, **Gulsvik A**, **Pillai SG**, **Silverman EK.** Variants in FAM13A are associated with chronic obstructive pulmonary disease. *Nat Genet* 42: 200–202, 2010. doi:10.1038/ng.535.
11. **Hancock DB**, **Eijgelsheim M**, **Wilk JB**, **Gharib SA**, **Loehr LR**, **Marciante KD**, **Franceschini N**, **van Durme YM**, **Chen TH**, **Barr RG**, **Schabath MB**, **Couper DJ**, **Brusselle GG**, **Psaty BM**, **van Duijn CM**, **Rotter JI**, **Uitterlinden AG**, **Hofman A**, **Punjabi NM**, **Rivadeneira F**, **Morrison AC**, **Enright PL**, **North KE**, **Heckbert SR**, **Lumley T**, **Stricker BH**, **O'Connor GT**, **London SJ.** Meta-analyses of genome-wide association studies identify multiple loci associated with pulmonary function. *Nat Genet* 42: 45–52, 2010. doi:10.1038/ng.500.
12. **Pillai SG**, **Kong X**, **Edwards LD**, **Cho MH**, **Anderson WH**, **Coxson HO**, **Lomas DA**, **Silverman EK**; **ECLIPSE and ICGN Investigators.** Loci identified by genome-wide association studies influence different disease-related phenotypes in chronic obstructive pulmonary disease. *Am J Respir Crit Care Med* 182: 1498–1505, 2010. doi:10.1164/rccm.201002-0151OC.
13. **Godinas L**, **Corhay JL**, **Henket M**, **Guiot J**, **Louis R**, **Moermans C.** Increased production of TGF-beta1 from sputum cells of COPD: relationship with airway obstruction. *Cytokine* 99: 1–8, 2017. doi:10.1016/j.cyto.2017.06.018.
14. **Hogg JC**, **Chu F**, **Utokaparch S**, **Woods R**, **Elliott WM**, **Buzatu L**, **Cherniack RM**, **Rogers RM**, **Sciurba FC**, **Coxson HO**, **Pare PD.** The nature of small-airway obstruction in chronic obstructive pulmonary disease. *N Engl J Med* 350: 2645–2653, 2004. doi:10.1056/NEJMoa032158.
15. **Perotin JM**, **Adam D**, **Vella-Boucaud J**, **Delepine G**, **Sandu S**, **Jonvel AC**, **Prevost A**, **Berthiot G**, **Pison C**, **Lebargy F**, **Birembaut P**, **Coraux C**, **Deslee G.** Delay of airway epithelial wound repair in COPD is associated with airflow obstruction severity. *Respir Res* 15: 151, 2014. doi:10.1186/s12931-014-0151-9.
16. **Takizawa H**, **Tanaka M**, **Takami K**, **Ohtoshi T**, **Ito K**, **Satoh M**, **Okada Y**, **Yamasawa F**, **Nakahara K**, **Umeda A.** Increased expression of transforming growth factor-beta1 in small airway epithelium from tobacco smokers and patients with chronic obstructive pulmonary disease (COPD). *Am J Respir Crit Care Med* 163: 1476–1483, 2001. doi:10.1164/ajrccm.163.6.9908135.
17. **Asano K**, **Shikama Y**, **Shoji N**, **Hirano K**, **Suzaki H**, **Nakajima H.** Tiotropium bromide inhibits TGF-beta-induced MMP production from lung fibroblasts by interfering with Smad and MAPK pathways in vitro. *Int J Chron Obstruct Pulmon Dis* 5: 277–286, 2010. doi:10.2147/copd.s11737.
18. **Milara J**, **Peiro T**, **Serrano A**, **Cortijo J.** Epithelial to mesenchymal transition is increased in patients with COPD and induced by cigarette smoke. *Thorax* 68: 410–420, 2013. doi:10.1136/thoraxjnl-2012-201761.
19. **Jiang Z**, **Lao T**, **Qiu W**, **Polverino F**, **Gupta K**, **Guo F**, **Mancini JD**, **Naing ZZ**, **Cho MH**, **Castaldi PJ**, **Sun Y**, **Yu J**, **Laucho-Contreras ME**, **Kobzik L**, **Raby BA**, **Choi AM**, **Perrella MA**, **Owen CA**, **Silverman EK**, **Zhou X.** A chronic obstructive pulmonary disease susceptibility gene, FAM13A, regulates protein stability of beta-catenin. *Am J Respir Crit Care Med* 194: 185–197, 2016. doi:10.1164/rccm.201505-0999OC.
20. **Heuberger J**, **Birchmeier W.** Interplay of cadherin-mediated cell adhesion and canonical Wnt signaling. *Cold Spring Harb Perspect Biol* 2: a002915, 2010. doi:10.1101/cshperspect.a002915.
21. **Huber AH**, **Nelson WJ**, **Weis WI.** Three-dimensional structure of the armadillo repeat region of beta-catenin. *Cell* 90: 871–882, 1997. doi:10.1016/s0092-8674(00)80352-9.
22. **van Amerongen R**, **Nusse R.** Towards an integrated view of Wnt signaling in development. *Development* 136: 3205–3214, 2009. doi:10.1242/dev.033910.
23. **Van Scoyk M**, **Randall J**, **Sergew A**, **Williams LM**, **Tennis M**, **Winn RA.** Wnt signaling pathway and lung disease. *Transl Res* 151: 175–180, 2008. doi:10.1016/j.trsl.2007.12.011.
24. **Xing Y**, **Takemaru K**, **Liu J**, **Berndt JD**, **Zheng JJ**, **Moon RT**, **Xu W.** Crystal structure of a full-length beta-catenin. *Structure* 16: 478–487, 2008. doi:10.1016/j.str.2007.12.021.
25. **Steiling K**, **van den Berge M**, **Hijazi K**, **Florido R**, **Campbell J**, **Liu G**, **Xiao J**, **Zhang X**, **Duclos G**, **Drizik E**, **Si H**, **Perdomo C**, **Dumont C**, **Coxson HO**, **Alekseyev YO**, **Sin D**, **Pare P**, **Hogg JC**, **McWilliams A**, **Hiemstra PS**, **Sterk PJ**, **Timens W**, **Chang JT**, **Sebastiani P**, **O'Connor GT**, **Bild AH**, **Postma DS**, **Lam S**, **Spira A**, **Lenburg ME.** A dynamic bronchial airway gene expression signature of chronic obstructive pulmonary disease and lung function impairment. *Am J Respir Crit Care Med* 187: 933–942, 2013. doi:10.1164/rccm.201208-1449OC.
26. **Gruenert DC**, **Basbaum CB**, **Welsh MJ**, **Li M**, **Finkbeiner WE**, **Nadel JA.** Characterization of human tracheal epithelial cells transformed by an origin-defective simian virus 40. *Proc Natl Acad Sci USA* 85: 5951–5955, 1988. doi:10.1073/pnas.85.16.5951.
27. **Cong L**, **Ran FA**, **Cox D**, **Lin S**, **Barretto R**, **Habib N**, **Hsu PD**, **Wu X**, **Jiang W**, **Marraffini LA**, **Zhang F.** Multiplex genome engineering using CRISPR/Cas systems. *Science* 339: 819–823, 2013. doi:10.1126/science.1231143.
28. **Ishikawa S**, **Ishimori K**, **Ito S.** A 3D epithelial-mesenchymal co-culture model of human bronchial tissue recapitulates multiple features of airway tissue remodeling by TGF-beta1 treatment. *Respir Res* 18: 195, 2017. doi:10.1186/s12931-017-0680-0.
29. **Popova AP**, **Bozyk PD**, **Goldsmith AM**, **Linn MJ**, **Lei J**, **Bentley JK**, **Hershenson MB.** Autocrine production of TGF-beta1 promotes myofibroblastic differentiation of neonatal lung mesenchymal stem cells. *Am J Physiol Lung Cell Mol Physiol* 298: L735–L743, 2010. doi:10.1152/ajplung.00347.2009.
30. **Tam A**, **Hughes M**, **McNagny KM**, **Obeidat M**, **Hackett TL**, **Leung JM**, **Shaipanich T**, **Dorscheid DR**, **Singhera GK**, **Yang CWT**, **Pare PD**, **Hogg JC**, **Nickle D**, **Sin DD.** Hedgehog signaling in the airway epithelium of patients with chronic obstructive pulmonary disease. *Sci Rep* 9: 3353, 2019. doi:10.1038/s41598-019-40045-3.
31. **Tam A**, **Wadsworth S**, **Dorscheid D**, **Man SF**, **Sin DD.** Estradiol increases mucus synthesis in bronchial epithelial cells. *PLoS One* 9: e100633, 2014. doi:10.1371/journal.pone.0100633.
32. **Leavitt B**, **Cullis P**, **Petkau T**, **Hill A**, **Wagner P**, **Kulkarni J.** Compositions and systems comprising transfection-competent vesicles free of organic-solvents and detergents and methods related thereto [Online]. The University of British Columbia, 2020. https://patents.google.com/patent/WO2020077007A1/#patentCitations
33. **Kulkarni JA**, **Darjuan MM**, **Mercer JE**, **Chen S**, **van der Meel R**, **Thewalt JL**, **Tam YYC**, **Cullis PR.** On the formation and morphology

of lipid nanoparticles containing ionizable cationic lipids and siRNA. *ACS Nano* 12: 4787–4795, 2018. doi:10.1021/acsnano.8b01516.

34. **Kulkarni JA**, **Witzigmann D**, **Leung J**, **van der Meel R**, **Zaifman J**, **Darjuan MM**, **Grisch-Chan HM**, **Thony B**, **Tam YYC**, **Cullis PR.** Fusion-dependent formation of lipid nanoparticles containing macromolecular payloads. *Nanoscale* 11: 9023–9031, 2019. doi:10.1039/c9nr02004g.
35. **Kulkarni JA**, **Thomson SB**, **Zaifman J**, **Leung J**, **Wagner PK**, **Hill A**, **Tam YYC**, **Cullis PR**, **Petkau TL**, **Leavitt BR.** Spontaneous, solvent-free entrapment of siRNA within lipid nanoparticles. *Nanoscale* 12: 23959–23966, 2020. doi:10.1039/D0NR06816K.
36. **Baarsma HA**, **Menzen MH**, **Halayko AJ**, **Meurs H**, **Kerstjens HAM**, **Gosens R.** beta-catenin signaling is required for TGF-beta1-induced extracellular matrix production by airway smooth muscle cells. *Am J Physiol Lung Cell Mol Physiol* 301: L956–L965, 2011. doi:10.1152/ajplung.00123.2011.
37. **Beyer C**, **Reichert H**, **Akan H**, **Mallano T**, **Schramm A**, **Dees C**, **Palumbo-Zerr K**, **Lin NY**, **Distler A**, **Gelse K**, **Varga J**, **Distler O**, **Schett G**, **Distler JH.** Blockade of canonical Wnt signalling ameliorates experimental dermal fibrosis. *Ann Rheum Dis* 72: 1255–1258, 2013. doi:10.1136/annrheumdis-2012-202544.
38. **Kulkarni JA**, **Witzigmann D**, **Chen S**, **Cullis PR**, **van der Meel R.** Lipid nanoparticle technology for clinical translation of siRNA therapeutics. *Acc Chem Res* 52: 2435–2444, 2019. doi:10.1021/acs.accounts.9b00368.
39. **Witzigmann D**, **Kulkarni JA**, **Leung J**, **Chen S**, **Cullis PR**, **van der Meel R.** Lipid nanoparticle technology for therapeutic gene regulation in the liver. *Adv Drug Deliv Rev* 159: 344–363, 2020. doi:10.1016/j.addr.2020.06.026.
40. **Corvol H**, **Rousselet N**, **Thompson KE**, **Berdah L**, **Cottin G**, **Foussigniere T**, **Longchampt E**, **Fiette L**, **Sage E**, **Prunier C**, **Drumm M**, **Hodges CA**, **Boelle PY**, **Guillot L.** FAM13A is a modifier gene of cystic fibrosis lung phenotype regulating rhoa activity, actin cytoskeleton dynamics and epithelial-mesenchymal transition. *J Cyst Fibros* 17: 190–203, 2018. doi:10.1016/j.jcf.2017.11.003.
41. **Massague J.** TGF-beta signal transduction. *Annu Rev Biochem* 67: 753–791, 1998. doi:10.1146/annurev.biochem.67.1.753.
42. **Zhou B**, **Liu Y**, **Kahn M**, **Ann DK**, **Han A**, **Wang H**, **Nguyen C**, **Flodby P**, **Zhong Q**, **Krishnaveni MS**, **Liebler JM**, **Minoo P**, **Crandall ED**, **Borok Z.** Interactions between beta-catenin and transforming growth factor-beta signaling pathways mediate epithelial-mesenchymal transition and are dependent on the transcriptional co-activator cAMP-response element-binding protein (CREB)-binding protein (CBP). *J Biol Chem* 287: 7026–7038, 2012. doi:10.1074/jbc.M111.276311.
43. **de Boer WI**, **van Schadewijk A**, **Sont JK**, **Sharma HS**, **Stolk J**, **Hiemstra PS**, **van Krieken JH.** Transforming growth factor beta1 and recruitment of macrophages and mast cells in airways in chronic obstructive pulmonary disease. *Am J Respir Crit Care Med* 158: 1951–1957, 1998. doi:10.1164/ajrccm.158.6.9803053.
44. **Duvernelle C**, **Freund V**, **Frossard N.** Transforming growth factor-beta and its role in asthma. *Pulm Pharmacol Ther* 16: 181–196, 2003. doi:10.1016/S1094-5539(03)00051-8.
45. **Chung KF.** Cytokines in chronic obstructive pulmonary disease. *Eur Respir J Suppl* 34: 50s–59s, 2001.
46. **Wang RD**, **Wright JL**, **Churg A.** Transforming growth factor-beta1 drives airway remodeling in cigarette smoke-exposed tracheal explants. *Am J Respir Cell Mol Biol* 33: 387–393, 2005. doi:10.1165/rcmb.2005-0203OC.
47. **Annes JP**, **Munger JS**, **Rifkin DB.** Making sense of latent TGFbeta activation. *J Cell Sci* 116: 217–224, 2003. doi:10.1242/jcs.00229.
48. **Cook D**, **Brown D**, **Alexander R**, **March R**, **Morgan P**, **Satterthwaite G**, **Pangalos MN.** Lessons learned from the fate of AstraZeneca's drug pipeline: a five-dimensional framework. *Nat Rev Drug Discov* 13: 419–431, 2014. doi:10.1038/nrd4309.
49. **Hobbs BD**, **de Jong K**, **Lamontagne M**, **Bosse Y**, **Shrine N**, **Artigas MS**; **COPDGene Investigators, et al.** Genetic loci associated with chronic obstructive pulmonary disease overlap with loci for lung function and pulmonary fibrosis. *Nat Genet* 49: 426–432, 2017. doi:10.1038/ng.3752.
50. **King EA**, **Davis JW**, **Degner JF.** Are drug targets with genetic support twice as likely to be approved? Revised estimates of the impact of genetic support for drug mechanisms on the probability of drug approval. *PLoS Genet* 15: e1008489, 2019. doi:10.1371/journal.pgen.1008489.
51. **Kim JH**, **Jang YS**, **Eom KS**, **Hwang YI**, **Kang HR**, **Jang SH**, **Kim CH**, **Park YB**, **Lee MG**, **Hyun IG**, **Jung KS**, **Kim DG.** Transforming growth factor beta1 induces epithelial-to-mesenchymal transition of A549 cells. *J Korean Med Sci* 22: 898–904, 2007. doi:10.3346/jkms.2007.22.5.898.
52. **Attisano L**, **Labbe E.** TGFbeta and Wnt pathway cross-talk. *Cancer Metastasis Rev* 23: 53–61, 2004. doi:10.1023/a:1025811012690.
53. **Warner DR**, **Greene RM**, **Pisano MM.** Cross-talk between the TGFbeta and Wnt signaling pathways in murine embryonic maxillary mesenchymal cells. *FEBS Lett* 579: 3539–3546, 2005. doi:10.1016/j.febslet.2005.05.024.
54. **Ziółkowska-Suchanek I**, **Mosor M**, **Podralska M**, **Iżykowska K**, **Gabryel P**, **Dyszkiewicz W**, **Słomski R**, **Nowak J.** FAM13A as a novel hypoxia-induced gene in non-small cell lung cancer. *J Cancer* 8: 3933–3938, 2017. doi:10.7150/jca.20342.
55. **Kent BD**, **Mitchell PD**, **McNicholas WT.** Hypoxemia in patients with COPD: cause, effects, and disease progression. *Int J Chron Obstruct Pulmon Dis* 6: 199–208, 2011. doi:10.2147/COPD.S10611.
56. **Vos PJ**, **Folgering HT**, **van Herwaarden CL.** Predictors for nocturnal hypoxaemia (mean SaO2 < 90%) in normoxic and mildly hypoxic patients with COPD. *Eur Respir J* 8: 74–77, 1995. doi:10.1183/09031936.95.08010074.
57. **Wang T**, **Larcher LM**, **Ma L**, **Veedu RN.** Systematic screening of commonly used commercial transfection reagents towards efficient transfection of single-stranded oligonucleotides. *Molecules* 23: 2564, 2018. doi:10.3390/molecules23102564.
58. **Baden LR**, **El Sahly HM**, **Essink B**, **Kotloff K**, **Frey S**, **Novak R**, et al. Efficacy and safety of the mRNA-1273 SARS-CoV-2 vaccine. *N Engl J Med* 384: 403–416, 2021. doi:10.1056/NEJMoa2035389.
59. **Polack FP**, **Thomas SJ**, **Kitchin N**, **Absalon J**, **Gurtman A**, **Lockhart S**, **Perez JL**, **Perez Marc G**, **Moreira ED**, **Zerbini C**, **Bailey R**, **Swanson KA**, **Roychoudhury S**, **Koury K**, **Li P**, **Kalina WV**, **Cooper D**, **Frenck RW, Jr.**, **Hammitt LL**, **Tureci O**, **Nell H**, **Schaefer A**, **Unal S**, **Tresnan DB**, **Mather S**, **Dormitzer PR**, **Sahin U**, **Jansen KU**, **Gruber WC**, **Group CCT**; **C4591001 Clinical Trial Group.** Safety and efficacy of the BNT162b2 mRNA Covid-19 vaccine. *N Engl J Med* 383: 2603–2615, 2020. doi:10.1056/NEJMoa2034577.
60. **Hu Y**, **Ng-Blichfeldt JP**, **Ota C**, **Ciminieri C**, **Ren W**, **Hiemstra PS**, **Stolk J**, **Gosens R**, **Konigshoff M.** Wnt/beta-catenin signaling is critical for regenerative potential of distal lung epithelial progenitor cells in homeostasis and emphysema. *Stem Cells* 38: 1467–1478, 2020. doi:10.1002/stem.3241.
61. **Kneidinger N**, **Yildirim AO**, **Callegari J**, **Takenaka S**, **Stein MM**, **Dumitrascu R**, **Bohla A**, **Bracke KR**, **Morty RE**, **Brusselle GG**, **Schermuly RT**, **Eickelberg O**, **Konigshoff M.** Activation of the WNT/beta-catenin pathway attenuates experimental emphysema. *Am J Respir Crit Care Med* 183: 723–733, 2011. doi:10.1164/rccm.200910-1560OC.